



**HAL**  
open science

## The Pyrenees: environments and landforms in the aftermath of the LGM (18.9–14.6 ka)

Magali Delmas, Yanni Gunnell, Marc Calvet, Théo Reixach, Marc Oliva

### ► To cite this version:

Magali Delmas, Yanni Gunnell, Marc Calvet, Théo Reixach, Marc Oliva. The Pyrenees: environments and landforms in the aftermath of the LGM (18.9–14.6 ka). *European Glacial Landscapes*, Elsevier, pp.185-200, 2023, 978-0-323-91899-2. 10.1016/B978-0-323-91899-2.00040-1 . hal-03989968

**HAL Id: hal-03989968**

**<https://univ-perp.hal.science/hal-03989968>**

Submitted on 28 Apr 2023

**HAL** is a multi-disciplinary open access archive for the deposit and dissemination of scientific research documents, whether they are published or not. The documents may come from teaching and research institutions in France or abroad, or from public or private research centers.

L'archive ouverte pluridisciplinaire **HAL**, est destinée au dépôt et à la diffusion de documents scientifiques de niveau recherche, publiés ou non, émanant des établissements d'enseignement et de recherche français ou étrangers, des laboratoires publics ou privés.

## **PART III. European glacial landforms during the main deglaciation (18.9–14.6 ka)**

### **SECTION 2 European regions that were not covered by the EISC**

#### **21. The Pyrenees: environments and landforms in the aftermath of the LGM (18.9–14.6 ka)**

**(Magali Delmas, Yanni Gunnell, Marc Calvet, Théo Reixach and Marc Oliva)**

**Abstract:** In the Pyrenees, the magnitude of ice fluctuations during the earlier part of the last glacial-to-interglacial transition (18.9–14.6 ka), or LGIT, is only well established for a dozen of small catchments, mostly on the basis of exposure ages. Constraints on the distribution and chronology of early LGIT glaciers in the eastern massifs have been used as proxies for palaeoclimatic reconstructions, with widespread evidence of rapid and extensive post-LGM deglaciation. In some Pyrenean valleys, such as in the upper Têt catchment, the LGM equilibrium-line altitude (ELA) rose from 2000–2100 m to ~2400 m as early as 19–20 cal ka BP. Thereafter, two glacier stillstands occurred around 19–18 ka and 17–16 ka. Glaciation patterns reveal systematically lower ELAs and higher glacier mass-balance gradients among massifs on the northern side of the range (thereby indicating cooler and wetter conditions) than on its southern side. These N–S climatic contrasts, still prominent today, have thus prevailed since the end of the LGM. In the central and western Pyrenees, data for the Noguera Ribagorçana, Noguera de Tor and Gállego valleys also document glaciers confined to the upper catchments around 17–16 ka.

**Key words:** last glacial-to-interglacial transition, stadial moraine, terrestrial cosmogenic nuclide exposure dating, climatic gradient, Pyrenees

##### **21.1. Introduction**

The Pyrenees form a 400-km-long and 80- to 130-km-wide continuous topographic barrier from the Atlantic to the Mediterranean. The highest elevations occur within a 140-km-long central segment between Mt. Balaitous and Pique d'Estats, where > 100 summits exceed 3000 m (highest summit: Aneto Peak, 3404 m). The more external belts attain lesser elevations of 1500–3000 m — with one exception: Monte Perdido, 3355 m — and are topographically more fragmented than the core of the orogen (Fig. 21.1). The modern climate of the Pyrenees hinges on two regional rainfall and temperature gradients, both relevant to understanding the Quaternary glacial context. The sharpest contrast opposes the cooler and moister oceanic climate of the northern slope, more directly influenced by the Atlantic Ocean, to the warmer and drier climate in the southern slope of the range, more strongly conditioned by the Mediterranean Sea. The climatic boundary approximately coincides with the orogen's summit ridgeline, but with strong local variations in the upper valleys where cols allowing Atlantic airstreams to spill southward into the Iberian domain (e.g., upper Ribagorça and Gállego). Conversely, the upper valleys of some north-flowing rivers are drier and sunnier than the regional average (e.g., upper Neste, Val d'Aran). The 0 °C isotherm in the central Pyrenees is now located at 2950 m (López-Moreno et al., 2019), although climate in the highest elevation belt is still poorly documented because weather stations are generally located in the valleys.

Glaciation today is residual. Glaciers covered an area of 320 ha in 2008 (2060 ha in 1850; René, 2013; Oliva et al., 2018) distributed among 27 dwindling cirque glaciers in 9 massifs of the central Pyrenees, all exceeding elevations of 3000 m except Mt. Valier (2838 m). The modern equilibrium-line altitude (ELA) ranges between 2500 and 3200 m, with variations dictated by topography-related local climatic conditions such as shading (north-facing aspect) and snow avalanching.

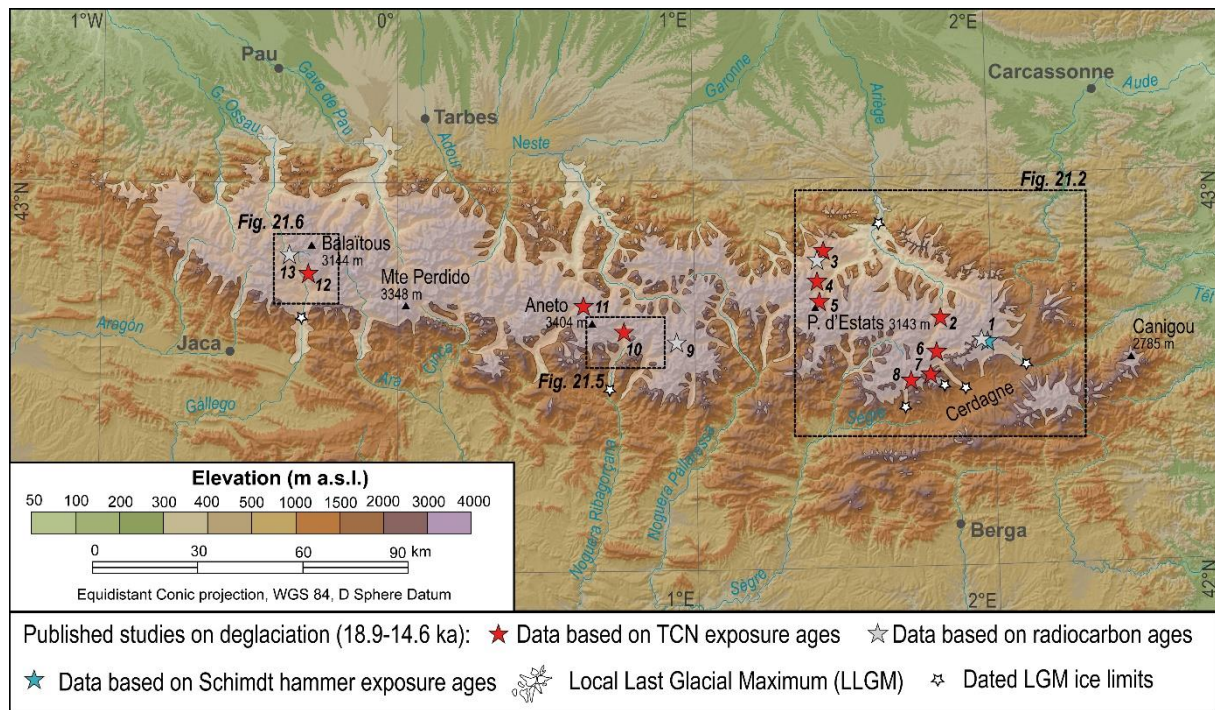


**Figure 21.1. Spatial distribution of published research on the early LGIT (18.9–14.6 ka) in the Pyrenees.** 1- Grave/upper Têt (Delmas, 2005; Delmas et al., 2008; Tomkins et al., 2018). 2- Upper Ariège (Delmas et al., 2011; Reixach et al., 2021). 3- Suc (Jalut et al., 1982; Delmas et al., 2011). 4- Escalé (Crest et al., 2017). 5- Picot (Jomelli et al., 2020). 6- Orri (Pallàs et al., 2010). 7- Malniu (Pallàs et al., 2010). 8- Arànsér and Llosa (Palacios et al., 2015a). 9- Noguera de Tor (Copons and Bordonau, 1996). 10- Noguera Ribagorçana (Pallàs et al., 2006). 11- Ésera (Crest et al., 2017). 12- Gállego (Palacios et al., 2015b, 2017). 13- Gállego (González-Sampéris et al., 2006; Guerrero et al., 2018).

The chronology of the Pleistocene glaciation has benefited from an increasing number of studies in recent years, but results in a majority concern the fluvio-glacial and ice-marginal landforms of the last most extensive glaciation (Delmas et al., 2022a, b, c). Glacier fluctuations during the earlier part of the last glacial-to-interglacial transition (early LGIT: 18.9–14.6 ka; on the Greenland chronostratigraphy: late GS-2.1b and full GS-2.1a, Rasmussen et al., 2014) are comparatively poorly documented, with only 12 valleys with dated ice-marginal deposits falling within that time window (Fig. 21.1).

During this period, valley glaciers receded deep into the mountain range and fragmented into numerous shorter valley and cirque glaciers, with their mass-balance gradients being increasingly controlled by local topographic and climatic conditions. Out of the dozen valleys currently documented, eight are located in the eastern Pyrenees (Fig. 21.2), thereby providing a fair density of data. The distribution of ice masses in this subregion is found to be a good proxy indicator of high-elevation climatic variability at local and regional scales, thereby also indirectly documenting changes

in atmospheric circulation during the LGIT over Western Europe and the Mediterranean (Reixach et al., 2021).

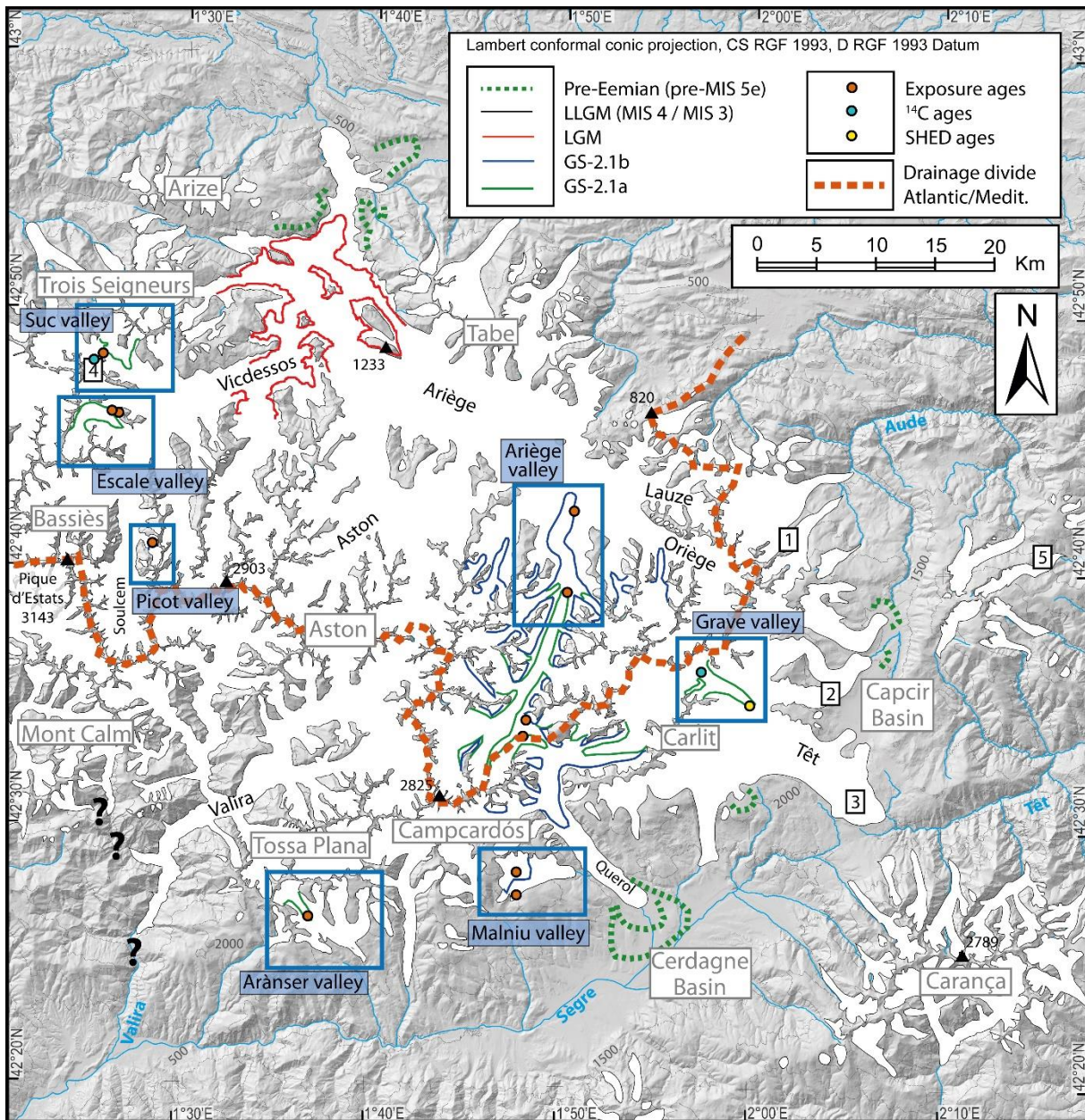


**Figure 21.2. Early LGIT ice extent in the eastern Pyrenees.** Blue rectangles locate the local glacial stades reported in Table 21.1. Numbered white squares locate the lacustrine sequences cited in the text: 1- Ruisseau de Laurenti; 2- Balcère; 3- La Borde; 4- Freychinède; 5- La Moulinasse.

## 21.2. The early LGIT in the eastern Pyrenees

### 21.2.1. Two stillstand positions in the upper Ariège valley during the early LGIT

The upper Ariège valley hosts four generations of post-LGM deposits documented between Ax-les-Thermes and the cirques (Fig. 21.2). Exposure ages obtained from the extant population of moraines indicate that they all formed during the LGIT, and the two older stillstands at Ax and Mérens coincide with the period between 18.9 and 14.6 ka (Fig. 21.2).

Ice-marginal deposits relating to the Ax stillstand provide a weighted mean age of  $18.0 \pm 0.5$  ka (i.e., end of GS-2.1b) based on 6 exposure ages on boulders ( $17.3 \pm 0.5$  ka without snow correction, Fig. 21.3A). At that time, the trunk glacier in the upper part of the catchment was 100 to 150 m thinner than during the LGM. Ice was nonetheless thick enough to allow the En-Garcia, Orri, Baladrar and Pas-de-la-Casa tributaries to join up as a unique composite glacier converging on Col de Puymorens (a diffluence col), and thereafter spilling north and south into the Ariège and Querol valleys, respectively. In the Ariège valley, the glacier was  $\sim 27.5$  km long and  $\sim 380$  m thick in the upper valley around Col de Puymorens, eventually thinning to 140 and 70 m near Ax-les-Thermes. On that basis, Reixach et al. (2021) modelled an ELA positioned at 2012 m, a mass-balance gradient of  $0.47 \pm 0.05 \text{ m}\cdot\text{yr}^{-1}\cdot 100 \text{ m}^{-1}$ , and best-fitting deviations from present-day reference conditions of  $-62 \pm 8\%$  for palaeoprecipitation (hereafter: P), and  $-9.7 \pm 0.5$  °C for palaeotemperature (hereafter: T).

The Ariège glacier retreated thereafter to a new stillstand position defined by the Mérens frontal moraines (Fig. 21.3B). In the upper part of the catchment, the Mérens stadial produced the lower right-margin moraine of the Vinyole complex, which documents a partial deglaciation of Col de Puymorens, and the right-margin boulder deposits (along the 2040 m elevation contour) of the Pas-de-la Casa glacier (Fig. 21.3C). The stillstand occurred around  $16.5 \pm 0.5$  ka, i.e., during GS-2.1a (weighted mean age based on 7 exposure ages from ice-marginal boulders, and without snow correction:  $15.7 \pm 0.5$  ka). At this time, the Ariège glacier was about 19.5 km long and 270 m thick (Pas-de-la-Casa valley), thickening to 300 m in the vicinity of the Vinyole frontal moraines. Reconstructed glaciological and paleoclimatic conditions indicate an ELA at 2152 m, a mass-balance gradient of  $0.50 \pm 0.05 \text{ m}\cdot\text{yr}^{-1}\cdot 100 \text{ m}^{-1}$ , and best-fitting P and T pairs of  $-44 \pm 16\%$  and  $-8.1 \pm 0.5$  °C, respectively (Reixach et al., 2021). The frontal positions of these two local stades lie, respectively, 30 and 38 km up-valley from the LGM moraines, and both correspond to a post-LGM ELA rise of 200 to 350 m (values in Table 21.1).

Pollen spectra documented from the lake sediments at Freychinède (1350 m), La Borde/La Borda (1660 m), Ruisseau de Laurenti (1860 m), Balcère/Vallsera (1770 m), and La Moulinasse (1360 m) confirm that climatic conditions for the early LGIT in the inner valleys of the eastern Pyrenees were very similar to those prevailing during the LGM (Fig. 21.2, synthesis in Jalut et al., 1992; Reille and Lowe, 1993). Until about 18 cal ka BP (i.e., end of GS-2.1b), plant assemblages were dominated by drought-tolerant steppe taxa (*Artemisia*, *Poaceae*, *Chenopodiaceae*); organic content in sediments and pollen counts were low, indicating overall sparse vegetation typical of cold continental climates with mean annual rainfall < 250 mm and fewer than 60 rainy days. After 18–17 cal ka BP, i.e., GS-2.1a, pollen concentrations and organic matter increased, with vegetation cover increasing to 10–30 % during GS-2.1b and to 60–80 % during GS-2.1a. The rise in *Pinus* and expansion of *Juniperus* in association with *Ephedra* on slopes more exposed to Mediterranean influence also document at that time a return to woodland vegetation. The persistence of herbaceous taxa throughout GS-2.1a nonetheless emphasises a prevalence of dry conditions (based on modern analogues where similar taxa thrive, and annual precipitation would have not exceeded 500 mm).

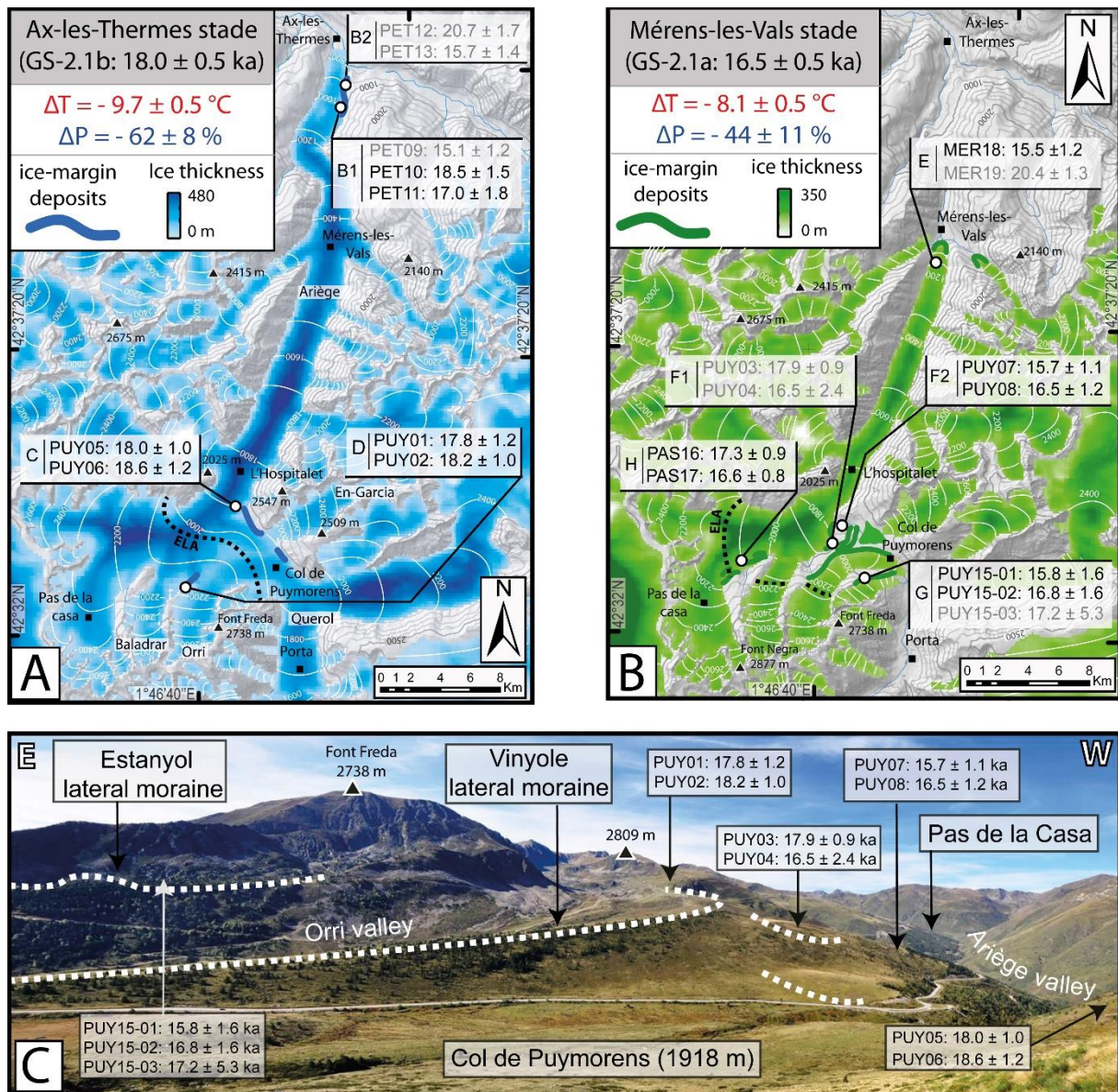


**Figure 21.3.** Early LGIT ice extent in the Upper Ariège valley (late GS-2.1b and GS-2.1a). A, B- Glacier configurations during the Ax and Mérens glacial stillstands (local stades) identified in the upper Ariège catchment. C- Sequence of ice-marginal deposits and  $^{10}\text{Be}$  exposures ages around Col de Puymorens. Exposures ages reported on the figure are calculated with snow correction factors of 0.95 for site C, 0.93 for site D, 0.94 for site F1, 0.96 for site F2, 0.93 for site G and 0.95 for site H. No snow shielding for sites B and E. Without correction for snow cover, exposure ages would be altered as follows for site C (PUY05:  $17.2 \pm 1.0$  ka; PUY06:  $17.7 \pm 1.1$  ka), site D (PUY01:  $16.6 \pm 1.1$  ka; PUY02:  $17.0 \pm 1.0$  ka), site F1 (PUY03:  $16.9 \pm 0.9$  ka; PUY04:  $15.6 \pm 2.3$  ka), site F2 (PUY07:  $15.2 \pm 1.0$  ka; PUY08:  $15.9 \pm 1.2$  ka), site G (PUY15-01:  $15.0 \pm 1.5$  ka; PUY15-02:  $15.6 \pm 1.5$  ka; PUY15-03:  $16.1 \pm 5.0$  ka), and site H (PAS16:  $15.9 \pm 0.8$  ka; PAS17:  $16.5 \pm 0.9$  ka).

### 21.2.2. Spatial variation of glaciation, with palaeoclimatic implications

Both of the early LGIT stadial stillstands recorded in the upper Ariège valley were also identified in other massifs of the eastern Pyrenees, but with more sites recording the 17–16 ka stillstand (GS-2.1a) than its 19–18 ka predecessor (GS-2.1b). Table 21.1 summarises the chronological, palaeogeographic, palaeoglaciological and palaeoclimatic data currently available for

the eastern Pyrenees between 18.9 and 14.6 ka. The record indicates a strong contrast between northern and more southern massifs in terms of glacier sizes, mass-balance gradients, ELA, and thus of palaeoclimatic conditions in the more elevated massifs of the range.

The upper Ariège valley hosted the longest glacier: 27.5 km at the end of GS-2.1b (Ax stade), and still 19.5 km during GS-2.1a (Mérens stade). Coeval glaciers on the south-facing sides of Campcardós (GS-2.1b: Malniu) and Tossa Plana (GS-2.1a: Arànsér) were just 2–3 km long, and a little longer (~6 km) on the south-facing slopes of the Carlit (GS-2.1a: La Grave) and Bassiès massifs (GS-2.1a: Légunabens) (Table 21.1). These size differences, however, are mostly explained by glacial catchment hypsometry in the accumulation zone rather than exclusively by contrasts in local palaeoclimate. It thus emphasises the notion that glacier length on its own can be a spurious proxy for palaeoclimate reconstruction compared to ELA and glacier mass-balance gradient, which integrate information more comprehensively about the regional climate and local (topoclimatic) effects.

With a surface area above the ELA of 90.7 km<sup>2</sup> at the time of GS-2.1b, and still 25.3 km<sup>2</sup> during GS-2.1a, the upper Ariège afforded by far the best conditions for hosting large glaciers during the early LGIT compared to < 4.4 km<sup>2</sup> in the other massifs of the eastern Pyrenees during the same period (Table 21.1). The spatial pattern of ELAs and mass-balance gradients reveal overall a general N–S contrast during the early LGIT, with lower ELAs and higher mass-balance gradients (and thus wetter conditions) among massifs on the north side of the Axial Zone. This pattern, still sharp and prominent today (cooler and wetter north), has thus prevailed for at least 19 ka, i.e., since the end of the LGM.

**Table 21.1. Glaciers in the eastern Pyrenees at the time of the early LGIT (18.9–14.6 ka)**

Location	Chronological data			Glaciological reconstructions				Palaeoclimatic reconstructions		
	Relative position within mountain range	INTIMATE ice stratigraphy (Rasmussen et al., 2014)	Local glacial stade	Age (ka ± 1 sigma)	Glacier length (km)	Area above ELA (km <sup>2</sup> )	ELA (m)	Mass-balance gradient (m.yr <sup>-1</sup> · 100 m <sup>-1</sup> )	ΔT (°C)	ΔP (%)
North			Ax-les-Thermes	18.0 ± 0.5	27.5	90.7	2012	0.47 ± 0.05	-9.7 ± 0.5	-62 ± 8
North	GS-2.1b		Outer Picot	17.8 ± 0.3	2.6	No data	2425 <sup>1</sup>	No data	No data	No data
South			Malniu	19.2 ± 0.7	3.1	2.1	2413	0.37 ± 0.06	-7.5 ± 0.5	-70 ± 9
North			Mérens-les-Vals	16.5 ± 0.5	19.5	25.3	2152	0.50 ± 0.05	-8.1 ± 0.5	-44 ± 11
North			Freychinède	16.7 ± 1.0	4.9	3.6	1700 <sup>1</sup>	0.65 ± 0.09	-9.1 ± 0.5 <sup>2</sup>	+45 ± 25 <sup>3</sup>
North			Légunabens	16.1 ± 0.2	6.6	4.4	2012	0.44 ± 0.05	-9.1 ± 0.5	-45 ± 11
North	GS-2.1a		Inner Picot	16.7 ± 0.1	1.9	0.4	2449 <sup>1</sup>	0.23 ± 0.04	-9.1 ± 0.5 <sup>2</sup>	-80 ± 5 <sup>3</sup>
South			Arànsér	Indirectly dated	2.4	0.5	2473	0.35 ± 0.05	-7.4 ± 0.5	-77 ± 7
South			Grave	16.1 ± 0.5	6.5	3.8	2383	0.40 ± 0.06	-7.5 ± 0.5	-67 ± 8

Notes. <sup>1</sup> ELA calculated using the AABR method (balance ratio of 1.59; Rea, 2009). <sup>2</sup> ΔT value obtained for Légunabens glacial stade. <sup>3</sup> ΔP value modeled on the basis of a ΔT value obtained from an adjacent catchment during the same glacial stade.

### 21.2.3. Post-LGM glacier recession and readvance in the Carlit massif

In addition to a succession of exposure-dated glacial landforms, the evolution of the upper Têt valley (known as La Grave, SE Carlit massif) is also documented by radiocarbon ages from a peat deposit (top of an in-situ sphagnum layer; elevation: 2150 m).  $^{14}\text{C}$  ages of 20–19 cal ka BP from the stratigraphy (Fig. 21.4) indicates that the valley glacier had already receded to the cirques by that time (Delmas, 2005; Delmas et al., 2008). The magnitude (~15 km) and celerity of post-LGM glacier recession in this valley are partly ascribable to catchment hypsometry. During the LGM, widespread plateau topography on the SE flank of the Carlit massif extended above the ELA and thus hosted an icefield able to feed three separate valley glaciers, each 15–20 km long. Towards the end of the LGM (ca. 19–20 cal ka BP), a rapid rise of the ELA (by 300–400 m) entailed the loss of this extensive contributing plateau area, thereby confining ice masses to the cirques at the very onset of the LGIT.

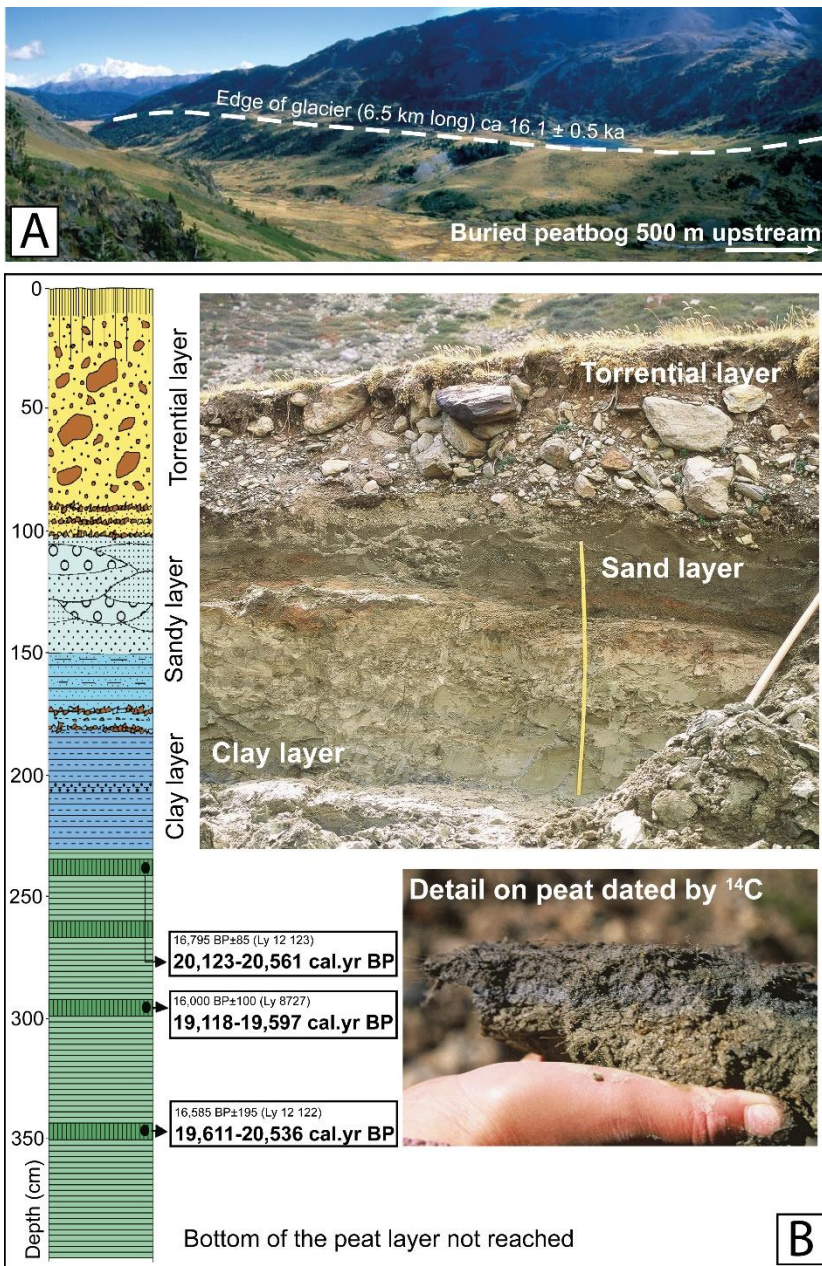


**Figure 21.4. Post-LGM deglaciation and early LGIT glacier readvance in the Grave valley.** A- Lateral moraine, legacy of the GS-2.1a glacial readvance in the Grave/upper Têt valley. B- Radiocarbon ages and stratigraphy of the buried peat bog and lacustrine, deltaic, and high-energy, poorly sorted fluvial deposits.

The hypsometric setting of the Carlit massif thus generated a large step change rather than a gradual change in glacier size at the onset of post-LGM warming. The ice-free portion of the valley was soon occupied by peat accumulations such as shown in Figure 21.4. A Schmidt-hammer-derived exposure age of  $16.1 \pm 0.5$  ka, obtained from boulders embedded in a frontal moraine situated  $\sim 3$  km down-valley from the peat deposit, has suggested nonetheless that the Grave glacier readvanced during GS-2.1a, thus overriding the peat-floored stratigraphy but preserving it (Tomkins et al., 2018). Based on a reconstructed ice-thickness profile for this short-lived stadial readvance, Reixach et al. (2021) modelled an ELA positioned at 2383 m, a mass-balance gradient of  $0.4 \text{ yr}^{-1} \cdot 100 \text{ m}^{-1}$ , and best-fitting palaeoclimatic magnitudes of  $-67 \pm 8\%$  (P), and  $-7.5 \pm 0.5$  °C (T) (Table 21.1).

The Grave valley thus recorded two successive glacier stillstands: (i) small glaciers confined to the cirques as early as 20 or 19 cal ka BP, followed by (ii) a readvance ca. 16 ka of the main trunk glacier (length: 6.5 km). ELA values in each case are imprecise and appear close ( $\sim 2400$  m initially, then  $\sim 2380$  m at the time of GS-2.1a), but they nonetheless document a readvance of this south-facing glacier. There is currently no independent evidence to corroborate the occurrence of either a glacial readvance or of climatic cooling in other catchments of the region, but the record nonetheless provides a preliminary hint that the 18.9–14.6 ka interval in the eastern Pyrenees was not just a steady succession of recessional stillstands: it also involved at least one short-lived event of glacier expansion.

### **21.3. The early LGIT in the central and western Pyrenees**

#### **21.3.1. Noguera de Tor and Noguera Ribagorçana**

The Noguera de Tor and Noguera Ribagorçana valleys each hosted composite glaciers during the LGM. Those glaciers may have only merged during occasional and short-lived periods. Both glaciers retreated to their upper valley areas after the LGM before readvancing during the early LGIT to positions well established in the Noguera Ribagorçana (Pallàs et al., 2006). The Santet moraine (1565 m) yielded a weighted mean age of  $17.5 \pm 1.7$  ka based on three exposure ages from different boulders (IST01:  $18.1 \pm 1.6$  ka, IST02:  $15.6 \pm 1.7$  ka, IST03:  $20.2 \pm 3.3$  ka, see Fig. 21.5 for exposure ages without snow correction). At that time (GS-2.1a), the upper Noguera Ribagorçana hosted a small composite glacier fed by two glaciers descending from the Mulleres (7 km) and Conangles (4 km) valleys; however, they were disconnected from the Besiberri glacier. The age of the Besiberri frontal moraine is more difficult to establish because exposure-age estimates were not obtained directly from moraine boulders. Age constraints were obtained instead from the glacially-polished bedrock steps situated below (OBS01:  $21.4 \pm 2.8$  ka) and above it (BES01:  $17.0 \pm 1.9$  ka). These two ages are nonetheless consistent with the respective positions of the dated rock surfaces in a recessional scenario, thus confirming that the Besiberri moraine is the legacy of a stationary glacier positioned between the two bedrock steps during the early LGIT. From this, it can be inferred that the Besiberri valley at the time was hosting a short glacier,  $\sim 2$  km long, descending to  $\sim 2000$  m and with an ELA situated between 2400 and 2500 m, i.e., 300 to 400 m higher than in the Mulleres and Conangles catchments where the ELA, at that time, was situated between 2050 and 2150 m (Table 21.2). This is a very large discrepancy in supposedly coeval ELAs between two neighbouring catchments. Such an anomaly in glacier behaviour calls for two possible explanations: (i) short-range contrasts in environmental constraints (hypsometry, topoclimatic conditions) imposing diverse glacier responses; or (ii) nuclide inheritance in the samples obtained from the glacially polished

bedrock surfaces, which would thus be yielding older face-value ages than expected for the Besiberri glacier (with the higher ELA).

**Table 21.2. Glaciers in the central and western Pyrenees at the time of the early LGIT (18.9–14.6 ka)**

Valley name (glacier name)	Glacier front elevation	Glacier length	ELA			Age of early LGIT deposits  (ka ± 1σ)	Key references
			THAR <sup>3</sup>	AAR <sup>6</sup>	AABR <sup>7</sup>		
	(m)	(km)	(m)	(m)	(m)		
N. Ribagorçana (Santet)	1565	4–7 <sup>1</sup>	2060– 2140 <sup>4</sup>	2039 ± 50	2089 ± 60	17.5 ± 1.7 ka (mean weighted <sup>10</sup> Be exposure ages from 3 boulders on Santet frontal moraine)	Pallàs et al., 2006
N. Ribagorçana (Besiberri)	2000	3	2320– 2400 <sup>4</sup>	2454 ± 50	2484 ± 60	21.4 ± 2.8 ka, 17.0 ± 1.9 ka ( <sup>10</sup> Be exposure ages from polished bedrock steps below and above the Besiberri moraine, respectively); see Fig. 21.5 and text for discussion	Pallàs et al., 2006
N. Ribagorçana (Besiberri)	1400	6–7 <sup>2</sup>		2150		14.9 ± 1.8 ka ( <sup>10</sup> Be exposure age from Hospital bedrock step covered by the reconstructed glacier); see Fig. 21.5 and text for discussion	Pallàs et al., 2006
N. de Tor (S. Nicolau)	No data	> 1		~2400		13.47 ± 0.06 <sup>14</sup> C ka BP (16,068–16,481 cal yr BP) (from base of glaciolacustrine sequence at Lake Redó, an indirect indication that the San Nicolau glacier was confined to the cirques during GS- 2.1a)	Copons and Bordonau, 1996
Ésera (Aigualluts)	2010	5–6	2480– 2560 <sup>5</sup>	2615 ± 50	2665 ± 50	16.2 ± 1.1 ka ( <sup>10</sup> Be exposure age from boulder, Aigualluts lateral moraine)	Crest et al., 2017
Ésera (L. del Hospital)	1740	10–11	2325– 2400 <sup>5</sup>	2487 ± 50	2487 ± 60	Exposure ages forthcoming	Unpublished
Gállego (Caldarés)	1200	10	1840– 1920 <sup>4</sup>	2284 ± 60	2284 ± 60	17.1 ± 1.5 ka ( <sup>10</sup> Be exposure age from boulder, Bolatica lateral moraine)	Palacios et al. 2015b, 2017

<sup>1</sup> Values for the Conangles and Mulleres catchments, respectively. <sup>2</sup> Value for the reconstructed glacier based on Harper and Humphrey (2003) and using an input ELA of 2150 m. <sup>3</sup> ELA calculated using the Toe-to-Headwall Altitude Ratio (THAR) method (ratio of 0.6). <sup>4</sup> Data calculated for ridgetop elevations of 2800 and 3000 m, respectively. <sup>5</sup> Data calculated for ridgetop elevations of 3200 and 3400 m, respectively. <sup>6</sup> ELA calculated using the Accumulation Area Ratio (AAR) method (ratio of 0.65 ± 0.05). <sup>7</sup> ELA calculated using the Area–Altitude Balance Ratio (AABR) methods (balance ratio of 1.59; Rea, 2009).

From an environmental perspective (hypothesis 1), the Besiberri catchment is relatively well shielded by the Posets–Maladeta massifs from Atlantic weather systems entering the area from the NW, whereas the Mulleres valley, on the southern side of Aneto Peak, benefits instead from high precipitation falling over the Maladeta — the highest massif in the Pyrenees. The resulting precipitation gradient could thus, perhaps, explain part of the observed ELA discrepancy. The coherence of the age data (hypothesis 2) was nonetheless also tested by running a simple glaciological model over the landscape under the constraints provided by the exposure-dated sequence of glacial landforms in the different valleys. In this simulation exercise (based on Harper and Humphrey, 2003), the modelled glaciers are forced to expand until they reach the desired spatial extent defined by the mapped and dated ice-marginal deposits, and a corresponding ELA is retrieved as a model output (Reixach et al., 2021). Alternatively, a desired ELA can be entered and the model produces the corresponding glaciation pattern. Results are shown in Figure 21.5.

Figure 21.5A shows that, for a uniform ELA set at 2150 m over the entire focus area, the Besiberri glacier would have been disconnected from the Santet glacier but would have descended all the way into the Ribagorçana trunk valley (terminal elevation: ~1400 m). Under this scenario, the

glacially-polished Hospitalet bedrock step (exposure age:  $14.9 \pm 1.8$  ka, RLH02) would have been covered by the Besiberri glacier at the time when the merging Mulleres and Conangles glaciers were generating the Santet moraine. While consistent with the Hospitalet bedrock exposure age, this scenario is not, however, consistent with the two bedrock-step exposure ages up- and downstream from the (undated) Besiberri moraine. Those results ( $17.0 \pm 1.9$  ka and  $21.4 \pm 2.8$  ka, respectively) are both too old to serve as reliable indicators of the Besiberri deglaciation chronology. Nuclide inheritance in the bedrock-step  $^{10}\text{Be}$  concentrations is thus a strong possibility and should be treated as a source of error in the Besiberri exposure ages.

Another scenario illustrated by Figure 21.5B shows that when the regional ELA is positioned at 2450 m (a value calculated for the Besiberri moraine based on the Accumulation Area Ratio method, see Table 21.2), the Conangles valley turns out to be entirely deglaciated whereas the Mulleres valley still hosts a 3-km-long valley glacier (descending to  $\sim 1700$  m). Given the exposure ages of  $13.5 \pm 2.2$  ka (MUL01) and  $13.6 \pm 1.5$  ka (MUL04) obtained in this valley segment (weighted mean:  $13.5 \pm 0.1$  ka), it then becomes a possibility under this second scenario that the Besiberri frontal moraine (elevation: 2000 m) fits an age more compatible with GI-1 or GS-1 rather than with GS-2. Further data from the area would be required to test this exploratory hypothesis.

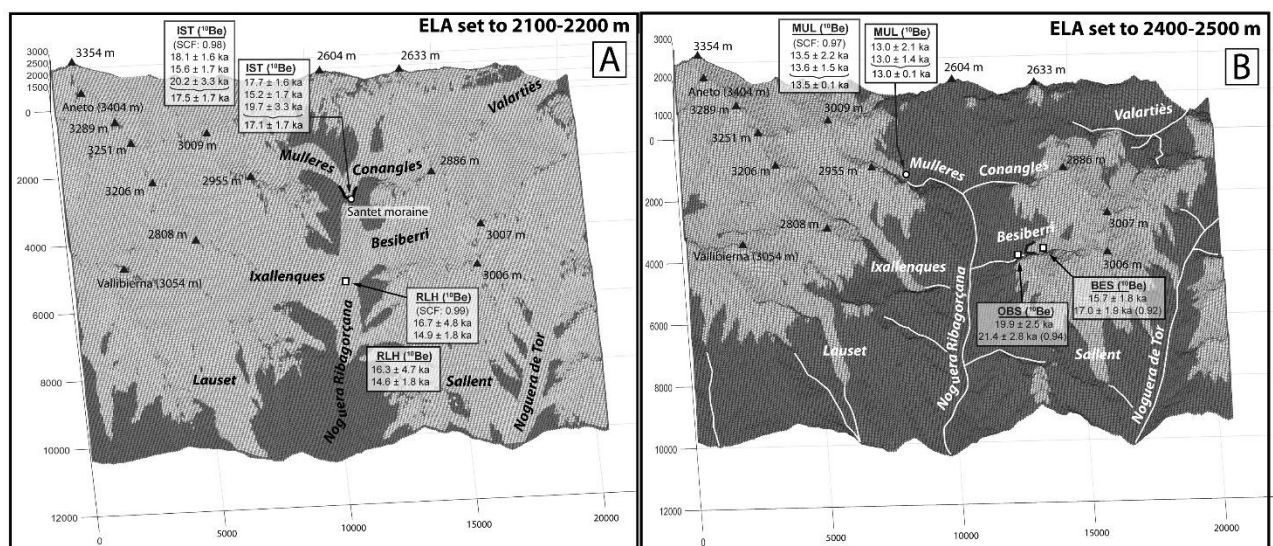


**Figure 21.5. Early LGIT ice extent in the Noguera Ribagorçana and Noguera de Tor.** Lighter tones: glaciated terrain; darker tones: deglaciated terrain. For samples IST, RLH and MUL, exposure ages with and without a snow correction factor (SCF values indicated in brackets) are presented in separate boxes, with weighted mean ages displayed below the curly bracket. For samples OBS and BES, exposure ages are reported without (top) and with (bottom) a snow correction factor (SCF values indicated in brackets). A- Ice extent modelled with an ELA positioned at 2150 m. Note that the reconstructed Besiberri glacier forms a diffluence lobe in the upstream direction of the low-gradient trunk valley. This occurs because the Harper and Humphrey (2003) model adjusts ice movement to climatic, glaciological and topographic conditions entered as initial settings (it was assumed, for example, that the present-day topography was a relevant proxy for the LGIT subglacial topography). This could be a model artefact, but it also has heuristic value because it could equally indicate the presence of previously undetected glaciolacustrine deposits in the vicinity of the lobe. Note, for example, that the gentle topography around the Noguera–Besiberri valley junction could derive from

*a kame deposit formed when the regional ELA was positioned around 2150 m (GS-2.1a: Santet glacial stillstand). B- Ice extent modelled for an ELA positioned at 2450 m. Note that the glaciers reconstructed on the basis of the Besiberri moraine (frontal moraine at 2000 m and ELA around 2050–2150 m) match the Mulleres glacial stillstand more accurately than the Santet stillstand. Distance from origin on X and Y axis in metres. Elevation in metres above sea level.*

Finally, the basal layer of a drill core into the lacustrine sediments of Lake Redó (elevation: 2110 m) yielded a radiocarbon age of  $13.47 \pm 0.06$  ka BP (16,068 to 16,481 cal yr BP, Copons and Bordonau, 1996). This evidence indicates that, by ca. 17,000 cal yr BP (GS-2.1a), glaciers were confined to the cirques of San Nicolau valley, a tributary of the Noguera de Tor, with an ELA around 2400 m (Copons and Bordonau, 1996). Such rapid and extensive deglaciation soon after the LGM is consistent with the hypsometry of the local catchment, which displays very few areas above 2400 m. It is also consistent with an observed tendency for the ELA to rise sooner to greater elevations in massifs sheltered from Atlantic weather systems. The extent of glaciers in the Noguera de Tor valley still remains poorly documented but the much larger catchment area above 2400 m suggests an accumulation zone large enough to sustain a fairly long trunk glacier during the early LGIT.

### **21.3.2. Garonne valley**

Although the Upper Garonne catchment hosted the longest glacier of the Pyrenees during the last glacial cycle, exposure ages from polished bedrock surfaces in the catchment's headwaters show that glaciers had already abandoned the Garonne valley floor by ~15 ka (ages between 14.8 and 14.2 ka in Bacivèr Cirque, 1950–2440 m; Oliva et al., 2021). Glacier thinning and recession was also detected ca.  $14.4 \pm 1.2$  ka (mean age) in neighbouring Saboredo Cirque, as revealed by four samples (ARAN-31:  $14.8 \pm 0.9$  ka, ARAN-34:  $14.0 \pm 0.8$  ka, ARAN-40:  $15.0 \pm 0.9$  ka, ARAN-39:  $13.8 \pm 0.8$  ka) from glacially-polished surfaces from the valley floor and the cirque edges (Fernandes et al., 2021). Further studies are needed to assess the evolution of the Garonne glacier between the LGM and the onset of the Bølling–Allerød interstadial.

### **21.3.3. Ésera valley**

A series of  $^{10}\text{Be}$  exposure ages (corrected for snow cover) were obtained for cirque glacier deposits in the Maladeta massif (Crest et al., 2017), but only one result from a lateral moraine at Plan des Aigualluts (Ésera valley, elevation: 2014 m) happens to be relevant to the early LGIT. The corresponding boulder exposure age of  $16.2 \pm 1.1$  ka ( $15.0 \pm 0.9$  ka without snow correction) implies that, during GS-2.1a, the Aneto and Barrancs cirques were feeding a 5–6 km-long glacier that descended to 2000 m a.s.l., but that was already disconnected from the Maladeta glacier. The Llanos del Hospital moraines, situated 5 km downstream, outline a glacial stillstand corresponding to a composite glacier fed by the entire population of north-facing Maladeta cirques (frontal moraine: ~1740 m). Given the difference between the ELA at that time (2400–2500 m) and the reconstructed ELA relevant to the Aigualluts stadial position (2600–2700 m), it is likely that the Llanos del Hospital glacial stillstand (exposure ages forthcoming) also records the early LGIT period.

### 21.3.4. Upper Gállego valley

The headwaters of the Gállego and Ossau rivers are documented by an exposure-age chronology focused on glacially-polished bedrock steps and moraine-related boulders (Palacios et al., 2015b, 2017). Within the large dataset, a  $^{36}\text{Cl}$  exposure age of  $17.1 \pm 1.5$  ka from a boulder embedded in a lateral moraine (PANTI-2) documents the extent of the GS-2.1a ice advance in the Caldarés catchment (see Fig. 21.6 for exposure ages without snow correction). At that time, the Caldarés catchment hosted an 11-km-long glacier terminating ca. 1200 m and associated with an ELA situated between 2200 and 2300 m.

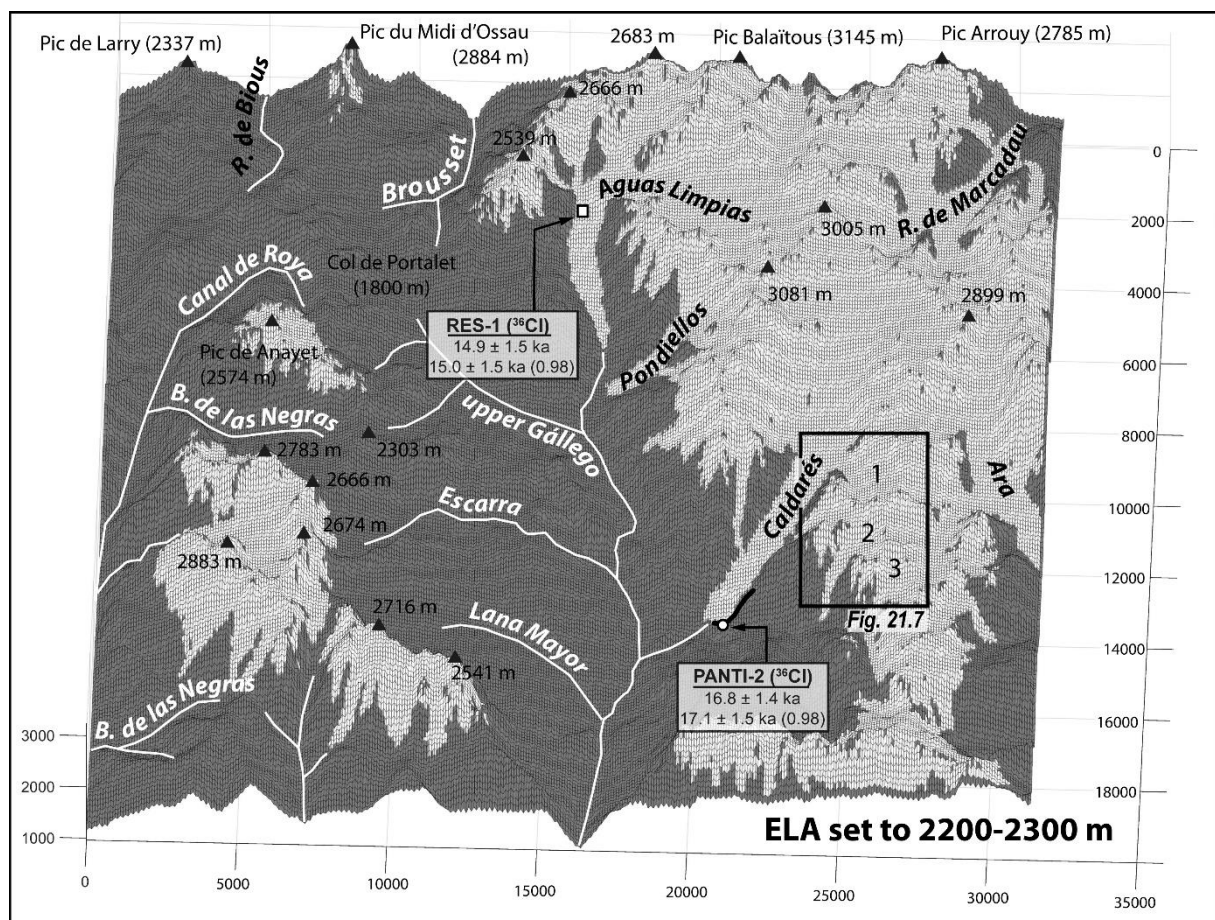


**Figure 21.6. Early LGIT ice extent in the Gállego catchment.** Lighter tones: glaciated terrain; darker tones: deglaciated terrain. Note that each exposure age is reported without (top) and with (bottom) a snow correction factor (SCF values indicated in brackets). Ice extent modelled with an ELA positioned at 2300 m. Note that the glaciers reconstructed on the basis of the Caldarés moraine (frontal position at 1200 m and ELA around 2300 m) corresponds to a ~10-km-long trunk glacier in the Aguas Limpias catchment. This reconstructed glacier matches the exposure age at  $15.0 \pm 1.5$  ka (RES-1) obtained in this valley at an elevation of 1525 m; the corresponding bedrock step was thus covered by ice at the time of GS-2.1a. 1- Brazato Cirque. 2- Piniecho Cirque. 3- Catieras Cirque. Distance on X and Y axis in metres. Elevation in metres above sea level.

Based on  $^{10}\text{Be}$  exposure ages of  $21.4 \pm 0.8$  ka and  $18.1 \pm 0.5$  ka on glacially-polished bedrock surfaces (BRAZA-1, BRAZA-2), Palacios et al. (2017) concluded that the Brazato cirque glacier was disconnected from the Caldarés glacier at the time of the GS-2.1a (see Fig. 21.7 for exposure ages without snow correction). Given, however, the hypsometry of the Brazato sub-catchment (cirque floor elevation: 2350–2400 m) and its topographic configuration opening directly into the Caldarés valley (see. Fig. 21.6), it is likely that BRAZA-1 and BRAZA-2 were still covered by a glacier at that time. As in the Noguera Ribagorçana (see Fig. 21.5 and attending Section 21.3.1), there is a strong possibility that  $^{10}\text{Be}$  concentrations measured from these bedrock samples display a component of nuclide inheritance (thereby generating anomalously old face-value exposure ages). In contrast, and following Palacios et al. (2017), we assume that glaciers at that time were confined to the Piniecho and Catieras cirque floors, in positions sheltered by high peaks (some exceeding 3000 m) from the influx of Atlantic moisture from the NW — a situation similar to the Besiberri glacier discussed in Section 21.3.1.  $^{10}\text{Be}$  and  $^{36}\text{Cl}$  exposure-dating constraints ( $n = 16$ ) on the moraines and rock glaciers hosted by those cirques indicate substantial age dispersal (Palacios et al., 2015b, 2017) but nonetheless show that the outermost moraines correspond to a stillstand that occurred during the early LGIT (Fig. 21.7). The Aguas Limpias catchment was hosting a glacier that extended far enough to cover the glacially-polished bedrock step located at spot elevation 2132 m. A  $^{36}\text{Cl}$  exposure age of  $15.0 \pm 1.5$  ka (RES-1) indicates the time elapsed since the glacier receded from that location (Palacios et al., 2015b, 2017). Meanwhile, the headwaters of the Gállego River (below Portalet pass, elevation: 2300 m) were already ice-free at the time of GS-2.1a (Fig. 21.6, González-Sampéris et al., 2006; Guerrero et al., 2018; Delmas et al., 2022c).

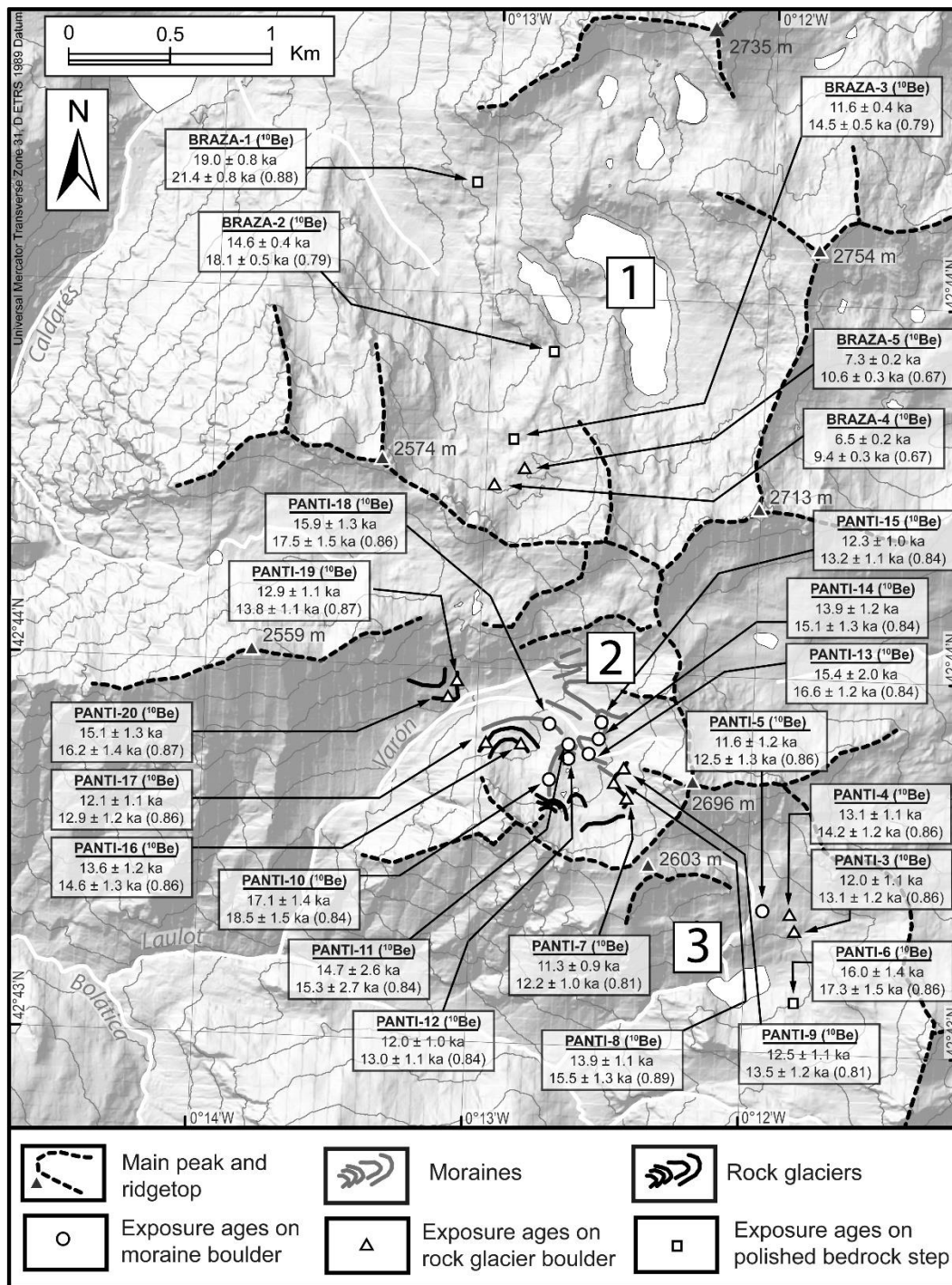


**Figure 21.7. Exposure ages in the Piniecho and Catieras cirques, Gállego catchment.** Note that each exposure age is reported without (top) and with (bottom) a snow correction factor (SCF values indicated in brackets). Base map (deposits, landforms and exposure ages) after Palacios et al. (2015b, 2017). 1- Brazato Cirque. 2- Piniecho Cirque. 3- Catieras Cirque. Snow correction factor in bracket. Digital elevation data source: Instituto Geográfico Nacional; ground resolution: 5 m.

## 21.4. Conclusions

Despite the limited number of age constraints on glacial landforms generated during the early LGIT (18.9–14.6 ka) (Fig. 21.1) — including controversial exposure-age interpretation issues at some sites — it appears that the behaviour of glaciers during this period was relatively uniform along

and across the Pyrenean range. The period recorded (i) rapid post-LGM glacier recession deep into the inner valleys, often as far as the ridgetop cirques; and (ii) a rise of ELAs by 200 to 300 m with respect to their LGM positions (Table 21.3).

**Table 21.3. Glaciated environments in the Pyrenees during the early LGIT (18.9–14.6 ka): a summary**

Valley (name of frontal moraine)	Climatic conditions relative to the LGM	Age of maximum glacier extent  (ka)	Proportion of ice cover (at maximum extent) relative to LGM  (%)	ELA at time of maximum extent  (m)	ELA change with respect to LGM  (m)	Glacier-front elevation at maximum extent  (m)	Main landforms	Key publications
<b>Upper Ariège</b> (Ax-les- Thermes)	Equally cold, but drier	19–18	25	2012	+200	750	Lateral and frontal moraines	Delmas et al., 2011; Reixach et al., 2021
<b>Upper Ariège</b> (Mérens)	Equally cold, but drier	17–16	12	2152	+300	1050	Lateral and frontal moraines	Delmas et al., 2011; Reixach et al., 2021
<b>Grave</b>	Equally cold, but drier	17–16	12	2383	+350	2030	Lateral moraines	Tomkins et al., 2018; Reixach et al., 2021
<b>Arànsér</b>	Equally cold, but drier	17–16	11	2473	No data	2215	Lateral and frontal moraines	Palacios et al., 2015a; Andrés et al., 2018; Reixach et al., 2021
<b>N. Ribagorçana</b> (Santet)	Equally cold, but drier	17–16	20	2100–2200	No data	1565	Frontal moraine	Pallàs et al., 2006
<b>Ésera</b> (Llanos del Hospital)	Equally cold, but drier	Forthcoming	22	2300–2400	No data	1735	Lateral and frontal moraines	Copons and Bordonau, 1997; Crest et al., 2017
<b>Gállego</b> (Caldarés)	Equally cold, but drier	17–16	20	~ 2300	+ 300	1200	Lateral moraines	Palacios et al., 2015b, 2017

Considering the persistence of very cold conditions throughout that time, it is likely that ELA shift was predominantly driven by increasing aridity, a feature well recorded by pollen diagrams (Jalut et al., 1992; Fletcher et al., 2010; Moreno et al., 2014) and by palaeoclimatic reconstructions based on glaciological models (Reixach et al., 2021). The legacy of depositional and erosional landforms of glacial origin produced in the Pyrenees during the LGIT enhances the potential for better understanding glacial oscillations during this period. Greater coverage from a wider range of massifs under distinct climatic regimes should eventually allow finer-scale documentation of ELA positions and fluctuations, and thus help to discriminate more accurately between local-scale and regional scale climatic causes of glacier behaviour at the end of the Pleistocene.

## References

- Copons, R., Bordonau, J., 1996. El registro sedimentario del cuaternario reciente en el lago Redó d'Aigües Tortes (Pirineos centrales). In: Grandal d'Anglade, A., Pagés Valcarlos, J. (Eds.), IV Reunión de Geomorfología, Sociedad Española de Geomorfología O Castro, 249–260.
- Copons, R., Bordonau, J., 1997. El último ciclo glaciar (Pleistoceno Superior–Holoceno) en el macizo de la Maladeta (Pirineos Centrales). *Revista de la Sociedad Geológica de España* 10, 55–66.
- Crest, Y., Delmas, M., Braucher, R., Gunnell, Y., Calvet, M., ASTER Team, 2017. Cirques have growth spurts during deglacial and interglacial periods: evidence from  $^{10}\text{Be}$  and  $^{26}\text{Al}$  nuclide inventories in the central-eastern Pyrenees (France, Spain). *Geomorphology* 278, 60–77.
- Delmas, M., 2005. La déglaciation dans le massif du Carlit (Pyrénées orientales): approches géomorphologique et géochronologique nouvelles. *Quaternaire* 16, 45–55.
- Delmas, M., Gunnell, Y., Braucher, R., Calvet, M., Bourlès, D., 2008. Exposure age chronology of the last glacial cycle in the eastern Pyrenees. *Quaternary Research* 69, 231–241.
- Delmas, M., Calvet, M., Gunnell, Y., Braucher, R., Bourlès, D., 2011. Palaeogeography and  $^{10}\text{Be}$  exposure-age chronology of Middle and Late Pleistocene glacier systems in the northern Pyrenees: implications for reconstructing regional palaeoclimates. *Palaeogeography, Palaeoclimatology, Palaeoecology* 305, 109–122.
- Delmas, M., Gunnell, Y., Calvet, M., Reixach, T., Oliva, M., 2022a. Glacial landscape of the Pyrenees (chapter 16). In: Palacios, D., Hughes, P., García-Ruiz, J.M., Andrés, A. (Eds.), *European Glacial Landscapes: Maximum Extent of Glaciations*. Elsevier, 123–128.
- Delmas, M., Gunnell, Y., Calvet, M., Reixach, T., Oliva, M., 2022b. The Pyrenees: glacial landforms prior to the Last Glacial Maximum (chapter 40). In: Palacios, D., Hughes, P., García-Ruiz, J.M., Andrés, A. (Eds.), *European Glacial Landscapes: Maximum Extent of Glaciations*. Elsevier, 295–307.
- Delmas, M., Gunnell, Y., Calvet, M., Reixach, T., Oliva, M., 2022c. The Pyrenees: glacial landforms from the Last Glacial Maximum (chapter 59). In: Palacios, D., Hughes, P., García-Ruiz, J.M., Andrés, A. (Eds.), *European Glacial Landscapes: Maximum Extent of Glaciations*. Elsevier 461–472.
- Fernandes, M., Oliva, M., Vieira, G., Palacios, D., Fernández-Fernández, J.M., Garcia-Oteyza, J., Schimmelpfennig, I., ASTER Team, Antoniades, D., 2021. Glacial oscillations during the Bølling–Allerød Interstadial–Younger Dryas transition in the Ruda Valley, Central Pyrenees. *Journal of Quaternary Science*, 1–17, <https://doi.org/10.1002/jqs.3379>.
- Fletcher, W.J., Sánchez Goñi, M.F., Allen, J.R.M., Cheddadi, R., Combourieu-Nebout, N., Huntley, B., Lawson, I., Londeix, L., Magri, D., Margari, V., Müller, U.C., Naughton, F., Novenko, E., Roucoux, K., Tzedakis, P.C., 2010. Millennial-scale variability during the last glacial in vegetation records. *Quaternary Science Reviews* 29, 2839–2864.
- González-Sampériz, P., Valero-Garcés, B., Moreno, A., Jalut, G., García-Ruiz, J.M., Martí-Bono, C., Delgado, A., Navas, A., Dedoubat, J.J., 2006. Climate variability in the Spanish Pyrenees during the last 30,000 yr revealed by the El Portalet sequence. *Quaternary Research* 66, 38–52.

Guerrero, J., Gutiérrez, F., García-Ruiz, J.M., Carbonel, D., Lucha, P., Arnold, L.J., 2018. Landslide-dam paleolakes in the Central Pyrenees, Upper Gállego River Valley, NE Spain: timing and relationship with deglaciation. *Landslides* 15, 1975–1989.

Harper, J.T., Humphrey, N.F., 2003. High altitude Himalayan climate inferred from glacial ice flux. *Geophysical Research Letters* 30, 1764–1767.

Jalut, G., Delibrias, G., Dagnac, J., Mardones, M., Bouhours, M., 1982. A palaeoecological approach to the last 21 000 years in the Pyrenees: The peat bog of Freychinède (Alt. 1350 m, Ariège, South France). *Palaeogeography, Palaeoclimatology, Palaeoecology* 40, 321–359.

Jalut, G., Montserrat, J., Fontugne, M., Delibrias, G., Vilaplana, J.M., Julia, R., 1992. Glacial to interglacial vegetation changes in the northern and southern Pyrenees: deglaciation, vegetation cover and chronology. *Quaternary Science Reviews* 11, 449–480.

Jomelli, V., Chapron, E., Favier, V., Rinterknecht, V., Braucher, R., Tournier, N., Gascouin, S., Marti, R., Galop, D., Binet, S., Deschamps-Berger, C., Tissoux, H., Aumaître, G., Boulès, D.L., Keddadouche, K., 2020. Glacier fluctuations during the Late Glacial and Holocene on the Ariège valley, northern slope of the Pyrenees and reconstructed climatic conditions. *Mediterranean Geoscience Reviews* 2, 37–51.

López-Moreno, J.I., Alonso-González, E., Monserrat, o., Del Río, L.M., Otero, J., Lapazaran, J., Luzi, G., Dematteis, N., Serreta, A., Rico, I., Serrano-Cañadas, E., Bartolomé, M., Moreno, A., Buisan, S., Revuelto, J., 2019. Ground-based remote-sensing techniques for diagnosis of the current state and recent evolution of the Monte Perdido Glacier, Spanish Pyrenees. *Journal of Glaciology* 65, 85–100.

Moreno, A., Svensson, A., Brooks, S.J., Connor, S., Engels, S., Fletcher, W., Genty, D., Heiri, O., Labuhn, I., Persoiu, A., Peyron, O., Sadori, L., Valero-Garcés, B., Wulf, S., Zanchetta, G., 2014. A compilation of Western European terrestrial records 60e8 ka BP: towards an understanding of latitudinal climatic gradients. *Quaternary Science Reviews* 106, 167–185.

Oliva, M., Ruiz-Fernández, J., Barriendos, M., Benito, G., Cuadrat, J.M., García-Ruiz, J.M., Giralt, S., Gómez-Ortiz, A., Hernández, A., López-Costas, O., López-Sáez, J.A., Martínez-Cortizas, A., Moreno, A., Prohom, M., Saz, M.A., Serrano, E., Tejedor, E., Trigo, R., Valero-Garcés, B., Vicente-Serrano, S., 2018. The Little Ice Age in Iberian mountains. *Earth-Science Reviews*, 177, 175–208.

Oliva, M., Fernandes, M., Palacios, D., Fernández-Fernández, J.M., Schimmelpfennig, I., ASTER Team, Antoniadou, D., 2021. Rapid deglaciation during the Bølling–Allerød Interstadial in the Central Pyrenees and associated glacial and periglacial landforms. *Geomorphology* 385, 107735.

Palacios, D., Gómez-Ortiz, A., de Andrés, N., Vázquez-Selem, L., Salvador-Franch, F., Oliva, M., 2015a. Maximum Extent of Late Pleistocene Glaciers and Last Deglaciation of La Cerdanya Mountains, Southeastern Pyrenees. *Geomorphology* 231, 116–129.

Palacios, D., de Andrés, N., López-Moreno, J.I., García-Ruiz, J.M., 2015b. Late Pleistocene deglaciation in the central Pyrenees: the upper Gállego valley. *Quaternary Research* 83, 397–414.

Palacios, D., García-Ruiz, J.M., Andrés, N., Schimmelpfennig, I., Campos, N., Léanni, L., ASTER Team, 2017. Deglaciation in the central Pyrenees during the Pleistocene-Holocene transition: Timing and geomorphological significance. *Quaternary Science Reviews* 162, 111–127.

Pallàs, R., Rodes, A., Braucher, R., Bourles, D., Delmas, M., Calvet, M., Gunnell, Y., 2010. Small, isolated glacial catchments as priority target for cosmogenic surface dating of Pleistocene climate fluctuations, SE Pyrenees. *Geology* 38, 891–894.

Pallàs, R., Rodés, A., Braucher, R., Carcaillet, J., Ortuno, M., Bordonau, J., Bourlès, D., Vilaplana, J.M., Masana, E., Santanach, P., 2006. Late Pleistocene and Holocene glaciation in the Pyrenees: a critical review and new evidence from  $^{10}\text{Be}$  exposure ages, south-central Pyrenees. *Quaternary Science Reviews* 25, 2937–1963.

Rasmussen, S.O., Bigler, M., Blockley, S.P., Blunier, T., Buchardt, S.L., Clausen, H.B., Cvijanovic, I., Dahl-Jensen, D., Johnsen, S.J., Fischer, H., Gkinis, V., Guillevic, M., Hoek, W.Z., Lowe, J.J., Pedro, J.B., Popp, T., Seierstad, I.K., Steffensen, J.P., Svensson, A.M., Vallelonga, P., Vinther, B.M., Walker, M.J.C., Wheatley, J.J., Winstrup, M., 2014. A stratigraphic framework for abrupt climatic changes during the Last Glacial period based on three synchronized Greenland ice-core records: refining and extending the INTIMATE event stratigraphy. *Quaternary Science Reviews* 106, 14–28.

Rea, B.R., 2009. Defining modern day area-altitude balance ratios (AABRs) and their use in glacier-climate reconstructions. *Quaternary Science Reviews* 28, 237–248.

Reille, M., Lowe, J.J., 1993. A re-evaluation of the vegetation history of the eastern Pyrenees (France) from the end of the Last Glacial to the Present. *Quaternary Science Reviews* 12, 47–77.

René, P., 2013. *Glacier des Pyrénées – Le réchauffement climatique en images*. Cairn (Pau), and Parc national des Pyrénées, 168 p.

Reixach, T., Delmas, M., Braucher, R., Gunnell, Y., Mahé, C., Calvet, M. 2021. Climatic conditions between 19 and 12 ka in the eastern Pyrenees, and wider implications for atmospheric circulation patterns in Europe. *Quaternary Science Reviews* 260, doi.org/10.1016/j.quascirev.2021.106923.

Tomkins, M.D., Dortch, J.M., Hughes, P.D., Huck, J.J., Stimson, A., Delmas, M., Calvet, M., Pallàs, R., 2018. Rapid age assessment of glacial landforms in the Pyrenees using Schmidt hammer exposure dating (SHED). *Quaternary Research* 90, 26–37.